Molecular Catalysis xxx (2017) xxx–xxx

Contents lists available at ScienceDirect

Molecular Catalysis

journal homepage: www.elsevier.com/locate/mcat

MCAT

Editor's choice paper

Application of 1,2,3-triazolylidene nickel complexes for the catalytic oxidation of *n*-octane

Siyabonga G. Mncube, Muhammad D. Bala*

School of Chemistry and Physics, University of KwaZulu-Natal, Private Bag X54001, Durban 4000, South Africa

ARTICLE INFO

Article history:
Received 7 December 2016
Received in revised form 26 February 2017
Accepted 6 March 2017
Available online xxx

Keywords:
Paraffin oxidation
n-Octane
Nickel complexes
Triazolium *N*-heterocyclic carbenes

ABSTRACT

Half-sandwich nickel complexes bearing a variety of mesoionic *N*-heterocyclic carbene ligands (η^5-cyclopentadienyl)-iodo-{1-(R)-3-methyl-4-phenyl-1H-1,2,3-triazol-3-ium-5-yl}nickel; where R = phenyl (**3a**); 2-ethoxy-2-oxoethyl (**3b**); propyl (**3c**); benzyl (**3d**) were synthesized by the reaction of nickelocene with the respective triazolium salts. The complexes were characterized by HRMS and multinuclear NMR, and the solid state structures of **3c** and **3d** were elucidated by single crystal X-ray diffraction analysis in which both complexes displayed a trigonal planar geometry. As catalysts for the oxidation of *n*-octane in the presence of oxidants under mild reaction conditions, all the complexes showed activity for the substrate yielding a range of oxygenated products. Under optimized reaction conditions, catalyst **3c** with lighter substituents on the triazolium ring exhibited the highest catalytic activity of 15% total conversion to products. With H_2O_2 as the more productive oxidant, the preferential activation of internal carbons led to the observation of a mixture of octanones as the dominant product stream of the oxidation reaction.

Introduction

N-Heterocyclic carbenes (NHC) have become one of the most popular supporting ligands in organometallic chemistry and homogeneous catalysis, due mainly to unique binding properties that make them superior to related two-electron donor ligands such as the ubiquitous phosphines [1–3]. The Arduengo-type imidazol-2-ylidenes dominate NHC chemistry because they are comparatively easy to prepare from readily available and affordable starting materials and have better stability than most phosphines [4,5]. However, limitations in their donating ability to transition metals, especially to highly reactive base metals (Fe, Co, Ni) has led to moves toward other heterocyclic azolium scaffolds that include triazolylidenes or so-called mesoionic carbene (mNHC) ligands [6]. This is related to the fact that 1,2,3-triazolylidenes are strong σ-donors that stabilise and provide access to highly reactive metal centres especially during catalysis [7,8]. In addition, the ease with which substituents around the triazole moiety may be fine-tuned to yield a myriad of ancillary mNHC ligands that display a wide variety of requisite properties has also added to the intense interest in the use of their metal complexes in catalysis [9,10]. In spite of all the interest, the isolation of metal-NHC complexes is non-trivial, and there are many synthetic techniques available for their preparation, of which the earliest and most utilised involves the preparation of "free" carbenes [11] that are subsequently reacted with metal precursors. However, concerns on the relative stability of "free" carbene ligands have resulted in the development of *in situ* approaches as alternative methods. Thus, the direct substitution of a labile basic metal bound ligand by a mNHC has been used as an effective strategy for the synthesis of triazolylidene transition metal complexes [12]. An example of this route developed by Cowley and co-workers [13] is the direct reaction of nickelocene with azolium salts to yield NHC-nickel complexes. Later, Albrecht and co-workers [14] adapted the method to the synthesis of mNHC-Ni complexes used in catalysis. In general, base metal complexes of this nature have demonstrated catalytic activity in a variety of reactions that include cross-coupling reactions [15,16], hydroarylation of alkynes [17] and enantioselective cyclopentane synthesis [18]. In much broader terms, NHC-metal complexes have been utilised in cross coupling reactions [19–21] and ring-closing metathesis [22] to mention just a few of their numerous applications. However, due to the relative inertness of saturated paraffin hydrocarbon C_{sp^3}–H bonds, the area of alkane oxidation has remained a challenge that is relatively unexplored [23,24]. Hence, as a continuation of our contributions [25–27] to the subject of paraffin oxidation using non-precious base metal complexes, we herein present the first use of mNHC-Ni complexes prepared via the direct (ligand substitution) route for the oxidation of *n*-octane under mild reaction conditions.

* Corresponding author.
E-mail addresses: bala@ukzn.ac.za, mdmdbala@gmail.com (M.D. Bala).

http://dx.doi.org/10.1016/j.mcat.2017.03.005
2468-8231/

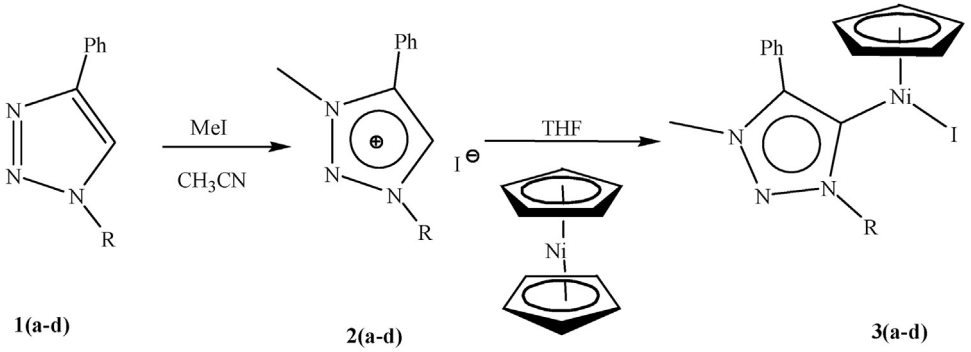

R = phenyl (**a**); ethyl propionate (**b**); propyl (**c**); benzyl (**d**)

Scheme 1. Synthesis of nickel complexes **3a–d**.

Results and discussion

Synthesis of triazolium nickel complexes

All the neutral triazoles and their corresponding salts were synthesized by reported methods via the well-established CuAAC 'click' protocols [28,29]. For the synthesis of the metal complexes, we adapted the method of Cowley and co-workers [13] developed for imidazolium ligand precursors to suit the triazolium compounds reported here. Hence, a series of the triazolium salts were treated with nickelocene in THF under reflux, a rapid colour change from deep green to reddish-violet was observed and noted as the first signs of ligand coordination and reaction between the carbene and the nickel centre. In this manner, the various synthesised ligand precursor salts (**2a–d**) were all successfully coordinated to nickel (**3a–d,** Scheme 1). The aim of this is to study the effects of both steric and electronic variations on the catalytic activity of the prepared metal complexes (*vide infra*).

The complexes were isolated from THF in good to excellent yields as violet crystalline solids, a clear improvement over earlier methods [30] that reported comparatively lower product yields when the reactions were conducted in dioxane. All the complexes were characterised by spectroscopic analysis and the solid-state structures of **3c** and **3d** were further analysed by single crystal X-ray diffraction. The compounds were all stable in air and only soluble in polar solvents, and ^{1}H NMR spectroscopic analysis of their solutions in $CDCl_3$ showed disappearance of the distinct characteristic triazolium C-5 proton that normally resonates around 9–10 ppm for uncoupled triazolium salts, suggesting successful deprotonation and ligand complexation to the Ni(II) centre. It should be noted that due to residual unreacted nickelocene, we initially encountered complications in assigning some NMR peaks due to abnormal chemical shifts, line broadening, and unusual signal integrations. This is similarly observed and documented in the literature [30,31], where some ^{1}H-NMR peaks assigned to the triazolium portion of the complexes were not fully resolved or became more complicated than expected. Following further purification and recrystallization, pure Ni-NHC complexes **3a–d** were confirmed. From the NMR data, the presence of an intense singlet peak at circa 5 ppm signifies the presence of one η^5-bonded cyclopentadienyl ligand. The NMR peak positions of the substituents on the bonded triazolium ligands were observed to in general have shifted slightly downfields when compared to the chemical shifts of corresponding uncoordinated salts (e.g. **3b** vs **2b**, supporting information).

The complexes were also characterised by ^{13}C NMR spectroscopy in which all the spectra indicated the presence of bonded triazolium ligands and a sharp peak resonating at circa 90 ppm assigned to the bonded Cp ligand clearly indicates formation of proposed half-sandwich complexes **3a–d** from nickelocene and the respective ligands. Observations from paraffin activation studies indicates that the incorporation of hydrophobic regions in the choice of ligand substituents is often favourable to catalytic efficiency of the complex in terms of alkane conversion to oxygenated products [26]. Hence, we attempted to extend the R substituent group (Scheme 1) to longer straight alkyl chains beyond propyl, but under the current reaction conditions, we only isolated traces of *trans*-ligated *bis*-carbene complexes which we believe resulted from the decomposition (double substitution or second carbene insertion) of the targeted half-sandwich complexes [30].

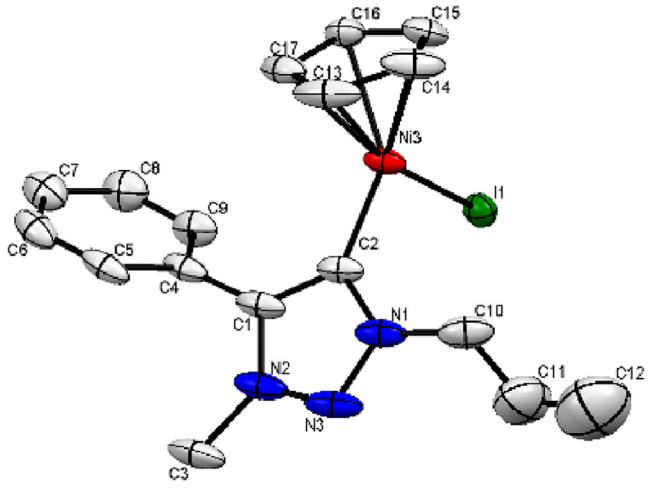

Fig. 1. ORTEP plot of complex **3c** with thermal ellipsoids drawn at the 50% probability level and hydrogen atoms omitted for clarity. Selected bond lengths (Å) and angles (°): Ni-I(1) = 2.4951(5); Ni-$C_{carbene}$ = 1.881(3); Ni-$Cp_{centroid}$ = 1.750(4); C(2)-Ni-I = 97.49(9); C(2)-Ni-$Cp_{centroid}$ = 131.28(6); I-Ni-$Cp_{centroid}$ = 131.18(4).

Violet single crystals of **3c** and **3d** suitable for X-ray diffraction studies were obtained from the slow diffusion of hexane into concentrated solutions of the complexes in dichloromethane. The molecular structures of **3c** and **3d** showing the connectivity of atoms in the complexes with important bond lengths and angles highlighted are shown in Figs. 1 and 2 respectively. Complex **3c** crystallised in the monoclinic *P21/c* space group while **3d** crystallised in the orthorhombic *Pna21*. With the cyclopentadienyl ring represented by a centroid, both complexes showed trigonal-planar coordination of the three ligands around each nickel(II) centre. Also, both structures clearly show the 1,3,4-distribution of substituents around each 1,2,3-triazolium ligand coordinated to the metal in a $C_{carbene}$-Ni fashion. The half-sandwich geometry incorporates the

Please cite this article in press as: S.G. Mncube, M.D. Bala, Application of 1,2,3-triazolylidene nickel complexes for the catalytic oxidation of *n*-octane, Mol. Catal. (2017), http://dx.doi.org/10.1016/j.mcat.2017.03.005

Table 1
Peroxide promoted catalytic oxidation of *n*-octane based on catalysts **3a–d**.[a]

Entry	Catalyst	Conversion (%)	Product distribution (%)			A/K ratio[b]
			ketones (4-;3-;2-)	alcohols (4-;3-;2-;1-)	aldehyde	acid	
1	Blank	2	100 (37; 21;42)	0	0	0	0.00
2	3a	10	63 (17:14:32)	26 (9;3;12;2)	7	4	0.41
3	3a-tBuOOH	4	39 (12;06;21)	57 (15;11;26;5)	4	0	1.46
4	3a-AcOH	7	54 (25;16;31)	19 (7;3;9;0)	2	7	0.35
5	3b	8	70 (22;12;36)	22 (5;4;13;0)	3	5	0.31
6	3c	15	64 (20;21;23)	28 (7;8;11;2)	5	3	0.44
7	3d	12	67 (21;16;30)	19 (6;3;9;1)	1	9	0.28

[a] Conditions for all reactions: solvent (MeCN) = 5 mL; *n*-octane = 0.84 M; oxidant (H_2O_2 or tBuOOH) = 14 mole equivalent; catalyst = 0.1 mol% (except entry 1 = none added); 80 °C; 24 h.
[b] A/K = relative ratio of total alcohol to total ketone products.

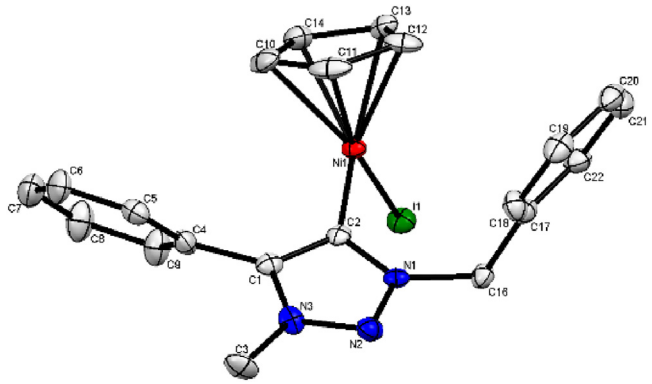

Fig. 2. ORTEP plot of complex **3d** with thermal ellipsoids drawn at the 50% probability level and hydrogen atoms omitted for clarity. Selected bond lengths (Å) and angles (°): Ni-I(1) = 2.5130(7); Ni-$C_{carbene}$ = 1.872(5); Ni-$Cp_{centroid}$ = 1.753(6); C(2)-Ni-I = 100.1(2); C(2)-Ni-$Cp_{centroid}$ = 127.25(4); I-Ni-$Cp_{centroid}$ = 132.72(7).

centroid of the cyclopentadienyl ligand as the mid-point between its five carbon atoms.

Major bond lengths and angles of both complexes are standard and no deviations of significance were observed in comparison with related compounds reported in the literature. This attests to the open nature of the coordination environment around the metal centre that allows for extensive ligand variability [13,30–32].

Application of compounds 3a-d as catalysts for the oxidation of n-octane

To test the efficiency of the prepared nickel complexes for the oxidation of *n*-octane we conducted a set of reactions aimed at studying any structure-activity relationships based on the chemical compositions of the catalysts. All experiments were conducted under similar conditions and initial results are presented in Table 1. Our main interest in paraffin oxidation research is the activation and functionalisation of readily available medium to light straight chain alkanes such as n-octane to value-added oxygenated products (octanols and octanones) under mild reaction conditions, which we aim to achieve using very common oxidants. The chemical inertness of the saturated alkane C—H bond limits the range of oxidants amenable to its activation and functionalisation. From a viewpoint of cost and environmental awareness, air and molecular oxygen (O_2) are the ideal oxidants, but the enthalpy requirement for their utilisation is inaccessible via the mild conditions utilised in this study. Hence, hydrogen peroxide (H_2O_2) and tertiary-butyl hydroperoxide (TBHP, tBuOOH) are the more commonly encountered in homogeneous alkane oxidation because the former is relatively cheap and only produce H_2O as by-product while the latter is more stable to decomposition by metal ions and its by-product hardly interferes with GC data analysis of the products. The H_2O_2 and TBHP oxidation of *n*-octane with the catalysts **3a–d** produced a mixture of isomeric 2-, 3- and 4- octanones and octanols as the major products (Scheme 2). CThe minor products (1-octanol, octanal and octanoic acid) all resulted from primary carbon (C1) activation and no cracking of the substrate was observed under the mild temperature conditions of 80 °C.

Table 1 shows the results of the catalytic testing beginning with a blank study (entry 1) in the absence of any metal additive, for which only 2% of mainly isomeric ketones was observed and no alcohols, products of C(1) activation or cracking were observed. Conversely, the addition of catalysts **3a–d** resulted in low to moderate conversions (4–15%) to oxygenated products in which production of ketones dominated over that of the alcohols with ratios of total alcohols/ketones (A/K) <1.

TBHP is a commonly utilised oxidant and in some cases preferred over H_2O_2 due to the greater stability of its active hydroperoxo species in catalysis when compared to H_2O_2 which easily decomposes to water and oxygen. As indicated by the results (entry 3), the adoption of tBuOOH has resulted in an improvement in selectivity to the alcohols (A/K >1.4), but the total conversion to oxygenated products was very low (4%) for further utilisation in the current study, hence the remainder of the reactions were conducted using H_2O_2 as the oxidant. This is an advantage for the current system since in comparison, H_2O_2 is considered a relatively 'greener' and environmentally benign oxidant. When an acid is added to oxidation reaction mixtures utilising H_2O_2 as the oxidant, a marked improvement in catalytic performance is usually observed. This improvement in catalytic performance of the acidified peroxide system has been attributed to stabilisation of the oxidant by the acid which slows down its decomposition to water and oxygen. Hence, we added acetic acid as a promoter to the reaction mixture (entry 4) and except for the early signs of catalyst decomposition no appreciable improvement in catalytic efficiency was recorded. In fact, for the current Ni catalysed reactions, the acetic acid may have accelerated the oxidation reaction, however during the course of the reaction we observed changes in the colour of the solution that may be attributed to catalyst decomposition which consequently

Please cite this article in press as: S.G. Mncube, M.D. Bala, Application of 1,2,3-triazolylidene nickel complexes for the catalytic oxidation of *n*-octane, Mol. Catal. (2017), http://dx.doi.org/10.1016/j.mcat.2017.03.005

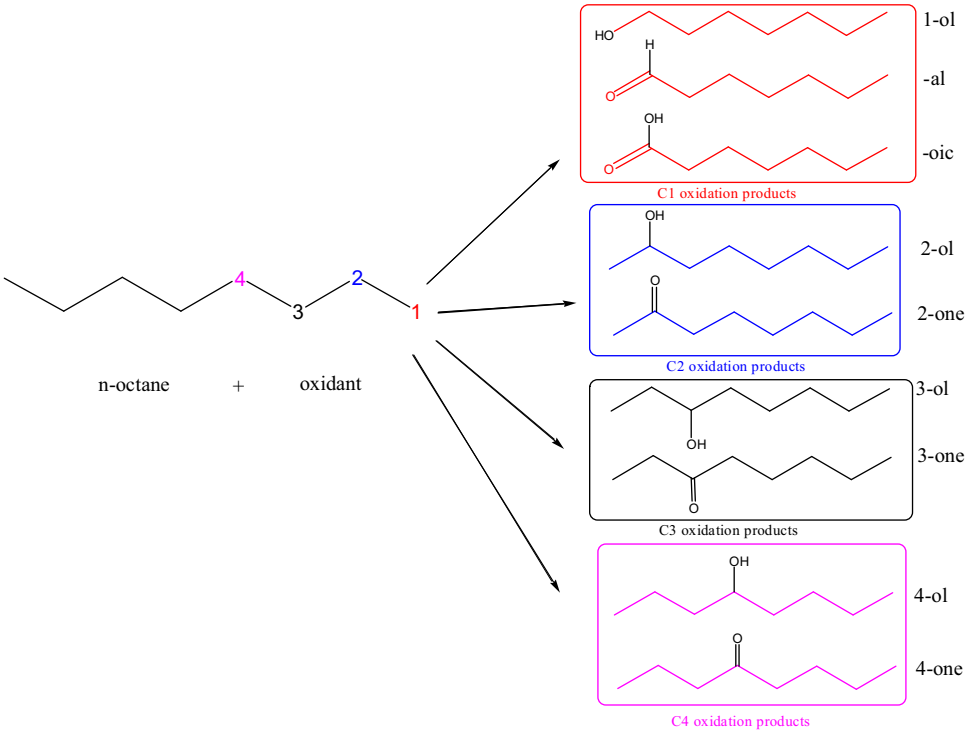

Scheme 2. Product distribution in the oxidation of *n*-octane.

led to overall reduction in its activity to only 7% total conversion to products compared to 10% conversion for the non-acidified system (entry 2).

In continuation, entries 5–7 respectively represent results for the variations in catalyst structure and molecular composition, mainly the effects of ring substituents of the triazolium ligand on the catalysis using the complexes **3b–d**. Systematic and gradual changes in electronic and steric influences of ligands around a metal ion are often invoked as tools in catalyst design for fine-tuning the catalytic efficiency of the metal with an overall aim of optimisation and improvement in efficiency. The results may be summarised thus:

- All the tested catalysts were active for the peroxide oxidation of *n*-octane with the ketones as the major product group (>50% total conversion to 2-, 3- and 4-one).
- This indicates that the catalysts are more selective to the activation and functionalization of internal methylene carbons [33]. See below for further discussion on product selectivity.
- Clearly, complex **3c** is the most active catalyst at a total conversion to products of 15%. We believe that the relatively higher activity of **3c** is due to the sterically less hindered propyl N-substituent which is also chemically more compatible with the substrate.
- Differences in electronic influence arising from variation in the composition of the ligands also play some role in determining the magnitude of catalytic activity of the tested complexes. For instance, the stark activity difference between **3a** and **3c** may be rationalised based on electronic differences of the ligands. Complex **3a** contains a set of phenyl groups as triazolium ring substituents, while **3c** is *N*-substituted with an electron donating propyl group. Hence, the delocalised aromatic electrons in **3a** rendered the ligand less nucleophilic with a negative influence on the metal centre and its catalytic activity.

In the oxidation of straight-chain *n*-alkanes, preferential functionalisation of the terminal C(1) carbon atoms is much desired over the functionalisation of internal carbons C(2, 3, etc.). This is best illustrated in biological systems where the hydrophobic region of enzymes was reported to be involved in the ready uptake, correct orientation and subsequent functionalization (hydroxylation) of C—H containing compounds selectively to primary alcohols and acids [33]. For the present set of complexes, analysis of products due to C(1) activation showed that catalyst **3c** exhibited the highest production of terminal oxidation products (octanal, 1-octanol and octanoic acid) in comparison to the other catalysts tested. It also showed higher selectivity towards the formation of alcohol products (with TBHP its A/K = 1.46) relative to the other catalysts. We believe that the presence of the hydrophobic alkyl chain substituent in the catalyst structure also contributed to the correct orientation of the *n*-octane chain for the preferential C(1) activation in **3c**.

However, in homogeneous solutions, due to numerous factors (nature of catalyst, solvent system, oxidants, etc.) straight-chain n-alkanes may adopt varying and continuously altering conformations [34,35] thus leading to poor selectivity and a mix-product stream. As illustrated in Scheme 2 for the functionalisation of *n*-octane with an atom of oxygen, depending on the position of attack and extent of oxidation, a total of nine oxygenated products are statistically possible. Hence, the concept of the regioselectivity parameter has become a useful tool for expressing the efficiency and selectivity of catalysts. The regioselectivity parameter for *n*-octane (C1:C2:C3:C4) is the relative reactivity at carbon positions 1, 2, 3, 4 respectively along its backbone and is used to analyse selectivity to the diversity of possible products in the oxidation reaction data. It represents the relative reactivity of the internal methylene (CH_2) hydrogen atoms normalised to the terminal methyl (CH_3) hydrogen atoms. Irrespective of type, the products are grouped together based on the position of the inserted oxygen, with normalisation carried out by dividing the total selectivity at each carbon by the number of hydrogens at that position (three for the terminal CH_3 and two for each unique internal CH_2). As a reference,

Please cite this article in press as: S.G. Mncube, M.D. Bala, Application of 1,2,3-triazolylidene nickel complexes for the catalytic oxidation of *n*-octane, Mol. Catal. (2017), http://dx.doi.org/10.1016/j.mcat.2017.03.005

Table 2
Site efficiency in the oxidation of *n*-octane by various catalyst systems.

System	C1:C2:C3:C4[a]	Reference
3a	1.0: 5.1: 2.0: 3.0	This work
3b	1.0: 9.1: 3.0: 5.0	This work
3c	1.0: 5.2: 4.4: 4.1	This work
3d	1.0: 5.3: 2.6: 3.6	This work
$Co[L]^{2+}$/TBHP[b]	1.0: 4.1: 3.3: 3.0	[25]
$[L_2Mn_2O_3](PF_6)_2/H_2O_2$[c]	1.0: 29.2: 25.5: 24.4	[36]
$[L_2Mn_2O_3](PF_6)_2/H_2O_2$[d]	1.0: 6.8: 5.9: 5.1	[36]
$[O\text{-}Cu_4\{N(CH_2CH_2O)_3\}_4(BOH)_4][BF_4]_2/H_2O_2$[e]	1.0: 5.1: 5.2: 4.3	[37]
$[O\text{-}Cu_4\{N(CH_2CH_2O)_3\}_4(BOH)_4][BF_4]_2$/TBHP[f]	1: 10: 6: 6	[37]
$NaVO_3\text{–}H_2SO_4/H_2O_2$[g]	1: 10.1: 10.7: 8.4	[38]
$Al(NO_3)_3/H_2O_2$[h]	1: 5.6: 5.6: 5.0	[39]

[a] Selectivity parameter C1:C2:C3:C4 is the normalized reactivity at carbon positions 1,2,3 and 4 respectively of the octane backbone with the reactivity at C(1) set to 1. Conditions for this study are the same as in Table 1.
[b] L = *bis*-tridentate-SNS-pyridine. MeCN, 80 °C, 24 h.
[c] L = 1,4,7-trimethyl-1,4,7-triazacyclononane. MeCN, 50 °C, 60 min.
[d] L = 1,4,7-trimethyl-1,4,7-triazacyclononane. UV irradiated, MeCN, 50 °C, 60 min.
[e] CF_3COOH, MeCN, 50 °C.
[f] MeCN, 50 °C.
[g] MeCN, 50 °C.
[h] MeCN, 70 °C.

the reactivity at the terminal carbon 1 is set to one. For this study, the selectivity parameter expressing total reactivity at each carbon atom is presented in Table 2. Also presented is the oxidation data for related systems for n-octane oxidation and for a full analysis and discussion on some of the systems presented in Table 2 see Ref. [25]. For a sample chromatogram displaying product distribution and analysis with catalyst **3c** see the ESI (Fig. S20).

In general, the data in Table 2 strengthens our initial observation that products of internal carbon oxidation (2-, 3- and 4-one & −ol, Scheme 2) especially the ketones predominate in the oxidation of n-octane. It is also clear that the terminal C(1) position is the least productive. It is worth noting that the accumulation of ketones in the oxidation reaction of alkanes has been shown to occur as a secondary process from the over-oxidation of alcohol products [25,37,40]. Minimising interaction between the initial alcohol products and the catalyst (oxidant) improves the A/K ratio and overall selectivity to alcohols. Hence, a possible explanation in favour of **3c** is that the presence of the short chain (hydrophobic) propyl group maximised the interaction between the substrate alkane and the catalyst to initially produce alcohols as the primary products while curtailing over-oxidation of the alcohols. In comparison, it is also obvious that the regioselectivity parameters for the oxidation of n-octane with H_2O_2 catalysed by our catalysts are comparable to those reported previously [25,36,41] suggesting that (i) our systems have followed similar mechanisms to those reported by Shul'pin and co-workers [37,42] and (ii) the conformations of n-octane have favoured oxidation of internal carbons especially C(2). This is because in all the systems listed in Table 2, functionalisation at the C(2) position is the most favoured oxidation site as reflected by the regioselectivity parameters.

Effects of variations in reaction conditions

At the onset, it is necessary to establish the optimum catalyst concentration based on the most active complex from the preliminary trial runs, i.e. complex **3c**. The molar concentration of the catalyst was varied between 0.05, 0.1, 0.2 and 0.5 mol%. Each run was monitored over a 24 hr period at the solvent reflux temperature of 80 °C. The results showed that as the catalyst concentration was doubled from 0.05 to 0.1 mol%, total conversion to oxygenated products also doubled (7–15%), which also happens to correspond to the highest turnover (TON = 150) recorded for the current catalyst system. However, as we ramped up the catalyst concentration to 0.5 mol%, no measurable increase in *n*-octane conversion was observed, except that the TON massively decreased. Hence all further optimisation studies were conducted at a 0.1% molar concentration of the most active catalyst **3c**.

Reaction temperature is a very important variable in most catalytic processes including paraffin oxidation reactions where it is often observed that catalytic productivity is temperature dependent. Fig. 3 presents the results of our investigation into the influence of reaction temperature on the current catalyst systems. Reactions were conducted in 5 mL MeCN using 0.84 M *n*-octane and 16 mole equivalent of the oxidant H_2O_2 and 0.1 mol% concentration of catalyst **3c** for a period of 24 h. The reaction temperature was gradually increased from 40 °C to the reflux temperature of the solvent (80 °C). It is important to note that earlier trial runs at room temperature indicated that no reaction occurred under all circumstances.

Fig. 3 shows that our results followed established trends in which total conversion of the substrate to the major oxidation products (octanones and secondary octanols) increased with increase in temperature. The test was conducted up to 80 °C in order to work within limits that ensure catalyst stability, controlled reflux of the solvent (acetonitrile) and well below the boiling point of the substrate *n*-octane [25,27]. Depending on the temperature used, different concentrations of isomeric alcohols and ketones were observed. At 40 °C comparable amounts of isomeric ketones and alcohols were obtained, however, the concentration of the alcohols gradually dropped with increase in temperature. Along the octane backbone, carbon position C(2) is the more reactive since it gave the highest combined concentration of products (2-ol and 2-one) while carbon C(1) is the least reactive. Also, products (formaldehyde and formic acid) associated with oxidation of the solvent acetonitrile were not observed in this study.

To determine the optimum reaction time, we conducted a set of reactions under reflux monitored at six hourly intervals (6, 12, 24 and 36 h). Other reaction conditions are similar to those presented above. The results showed that in the first 6 h, isomeric alcohols and ketones are the major products, however, after 24 h the concentration of alcohols has diminished significantly. Slow accumulation of ketones was also observed within the first 12 h, but after 24 h the rate of their formation was faster. This is most likely due to further oxidation of the alcohols by H_2O_2 to afford the corresponding ketones leading to a reduction in the molar concentrations of the alcohols relative to the ketones (reduction in A/K ratio). Hence all the optimised catalytic tests reported here were conducted over 24 h reaction period. It is well established that in catalytic processes

Please cite this article in press as: S.G. Mncube, M.D. Bala, Application of 1,2,3-triazolylidene nickel complexes for the catalytic oxidation of *n*-octane, Mol. Catal. (2017), http://dx.doi.org/10.1016/j.mcat.2017.03.005

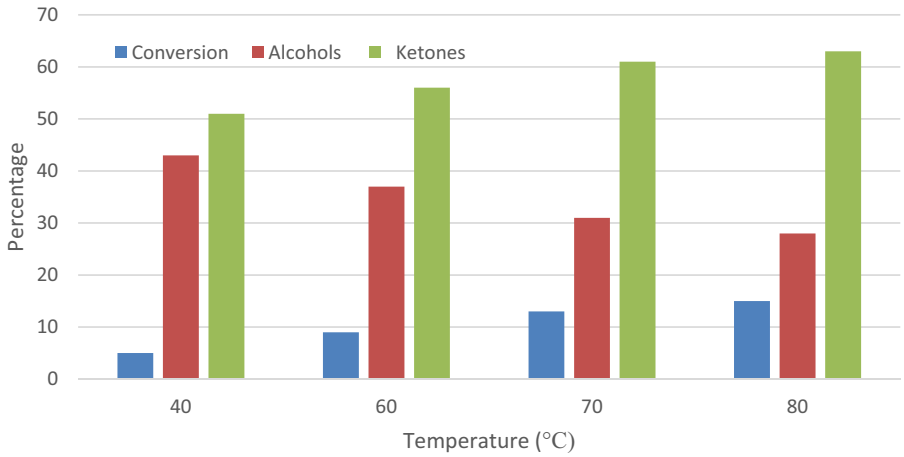

Fig. 3. Effect of temperature on selectivity to major products in the oxidation of n-octane with catalyst **3c**.

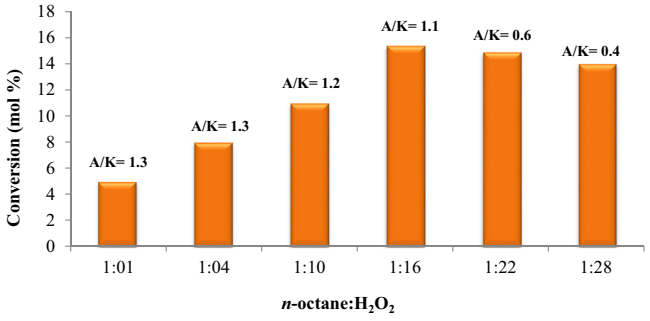

Fig. 4. Effects of variation in oxidant quantities on the oxidation of *n*-octane catalysed by complex **3c**.

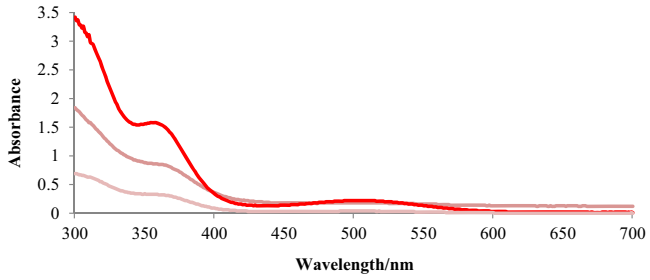

Fig. 5. Time dependent UV–vis spectral changes following the addition of H_2O_2 to a solution of **3c** in acetonitrile at 80 °C. Top (60 min), mid (4 h), bottom (16 h).

under an oxidising environment, alcohol products (which are easier to oxidise than the substrate alkane) often react further to yield corresponding ketones or acids [40].

Further, we also studied the effect of variation in the relative quantity of the oxidant H_2O_2 to the substrate. This was varied from 1:1 to 1:28 (mole/mole) and the results (Fig. 4) indicate that the yield of products increased with increase in the relative ratio of substrate to oxidant up to a maxima at 1:16. The proportion of the alcohol products (lower A/K ratio) was observed to drastically drop beyond this ratio, hence all other reactions were conducted with the relative amount of oxidant capped at 1:16.

Catalyst stability in an oxidising environment (without *n*-octane) was studied using time dependent UV/vis spectroscopy to detect any spectral changes due to structural transformations of the catalyst. The most active complex **3c** was used as a representative catalyst under similar conditions as the catalytic runs. The result is presented in Fig. 5, where no sign of change was observed within the first 60 min (top spectrum). However, after 4 h (middle spectrum), the solution gradually changed from bright red to reddish-brown, and the UV/vis spectrum showed a drop in intensity of absorbance (λ_{max} = 357 nm) which might be due to the onset of catalyst decomposition [43] or the formation of active intermediates [44]. From the product distribution profiles (Table 2), it is obvious that the most obvious active intermediates for this oxidation reaction are metal-oxo and −peroxo species [40,41], hence octyl hydroperoxide was the major product prior to its reduction by PPh_3. Also, these results agree with our earlier observations that no oxygenated products (or very negligible) were observed during the early stages of the reaction. It is also interesting to note that a measurable intensity of absorbance in the UV/vis spectrum persisted up to 16 h of reaction time (bottom spectrum), most probably indicating the availability of the active specie albeit at a diminished concentration, this is accompanied by a further change in colour of the solution to a light brown hue. After 48 h, the solution colour has completely changed into light brownish colour with a greenish paste-like precipitate (most probably nickel oxide).

In summary, it is obvious from all the data presented that a fine balance exists between product distribution (selectivity) and substrate conversion. This balance hinges on both the time of reaction and the relative amount of the oxidant. Shorter reaction times yielded more alcohol products albeit at low substrate conversions which is also supported by the use of relatively low quantity of the oxidant (up to 1:16). The catalyst is also shown to gradually transform in an oxidising environment, but remain relatively stable up to a period of 16 h.

Conclusions

1,2,3-Triazolium-based nickel carbene complexes (**3a**–**3d**) were synthesised by modification of reported synthetic methods. The crystal structures of two new Cp-Ni-NHC complexes were reported and discussed. All the complexes were applied for the catalytic oxidation of *n*-octane in the presence of oxidants under mild reaction conditions. All complexes were found to be active as catalysts and at the optimum reaction conditions, ketones were observed as the major product group. Overall, the catalyst system with a hydrophobic alkyl chain substituent (**3c**) in the catalyst structure yielded the highest substrate conversion of 15 mol% at a turnover of 150.

Experimental

Toluene and THF were dried over sodium wire and benzophenone, dichloromethane (DCM) was dried over phosphorous

Please cite this article in press as: S.G. Mncube, M.D. Bala, Application of 1,2,3-triazolylidene nickel complexes for the catalytic oxidation of *n*-octane, Mol. Catal. (2017), http://dx.doi.org/10.1016/j.mcat.2017.03.005

pentoxide. All solvents were freshly distilled before used. High purity nitrogen gas was purchased from Afrox. Glassware was oven dried at 110 °C. Triazoles **1a**–**d** and their corresponding salts **2a**–**d** were synthesised as described in published literature and all their characterisation data are consistent with the literature reports [28,29,45]. Amongst the catalysts, only complex **3a** was previously reported by Albrecht and co-workers [30], for which we also obtained similar spectroscopic, analysis and single crystal XRD data. All NMR experiments were done using a 400 MHz Bruker ultrashield spectrometer and samples were dissolved in deuterated solvents. Chemical shifts (δ) in ppm were reported with respect to tetramethylsilane (TMS) as internal standard. The following abbreviations were used to describe peak splitting patterns when appropriate: br = broad, s = singlet, d = doublet, t = triplet, q = quartet, m = multiplet. Infrared spectra (FTIR) were recorded on a Perkin Elmer FT-IR 1600 spectrophotometer.

General procedure for synthesis of [(η^5-Cp)I(mNHC)Ni(II)] complexes

The reported method [13] was modified: Under N_2 atmosphere, triazolium salts **2a**–**d** (1 equiv.) and $NiCp_2$ (1 equiv.) were charged into a flame-dried Schlenk tube and THF (20 mL) was added. The resultant mixture was heated to reflux at 70 °C for 24 hr to give a red solution in which a large brown insoluble solid was suspended. The solvent was evaporated under reduced pressure and the crude product was extracted with hot toluene and filtered through a bed of Celite.

The crude product was then purified by column chromatography (ethyl acetate: diethyl ether, 1:4) to give a reddish solid product. The same procedure was used to prepare all the Ni-NHC complexes (**3a**–**3d**) in good yields, details below:

(η^5-Cyclopentadienyl)-iodo-(3-methyl-1,4-diphenyl-1H-1,2,3-triazol-3-ium-5-yl)-nickel
(3a)

The starting materials used: 3-methyl-1,4-diphenyl-1H-1,2,3-triazol-3-ium iodide (0.80 g, 2 mmol) and $NiCp_2$ (0.41 g, 2 mmol). Reddish powder (0.78 g, 73%). Crystals suitable for X-ray crystallography were grown by layering hexane on dichloromethane. ^{1}H NMR ($CDCl_3$ 400 MHz) δ 7.17-7.54 (bm, Ar), 4.81 (s, Cp), 2.92 (s, N-CH_3), ^{13}C NMR ($CDCl_3$, 400 MHz):148.5, 130.7, 129.9, 129.8, 129.7, 129.1, 128.7, 128.4, 128.3, 128.0, 125.8, 120.5, 117.7, 91.8, 37.9.IR νmax (cm^{-1}): 3054 (m) 2922 (m), 2853 (m), 1695 (m), 1593 (m), 1400(m), 1042 (m), 917(m), 756 (s), 607 (s), 513 (m). HRMS (ESI) m/z for $C_{20}H_{18}N_3Ni$ [M−I]: calculated: 358.0854, found: 358.0866.

(η^5-Cyclopentadienyl)-iodo-{1-(2-ethoxy-2-oxoethyl)-3-methyl-4-phenyl-1H-1,2,3-triazol-3-ium-5-yl}nickel
(3b)

The starting materials used:1-(2-ethoxy-2-oxoethyl)-3-methyl-4-phenyl-1H-1,2,3-triazol-3-ium iodide (0.81 g, 2 mmol) and $NiCp_2$ (0.41 g, 2 mmol). Reddish solid product (0.71 g, 66%). ^{1}H NMR ($CDCl_3$ 400 MHz): δ 7.26-7.92 (bm, Ar), 5.21 (s, Cp), 4.33 (s, CH_2), 4.29 (s, N-CH_3), 1.13-1.33 (m, 5H, CH_2 +CH_3); ^{13}C NMR ($CDCl_3$ 400 MHz): δ 166.2, 148.2, 130.3, 129.1, 128.8, 125.8, 120.9, 96.0, 62.4, 50.39, 22.6, 11.4. IR ν_{max} (cm^{-1}): 3429 (b), 2929(m), 2360 (m), 1730 (b), 1616 (m), 1464 (m), 1370 (m), 1213 (b), 1025(s), 765(s), 695 (s), 502(m). HRMS (ESI) m/z for $C_{18}H_{20}N_3NiIO_2$ [M]: calculated: 497.0954, found: 497.0934.

(η^5-Cyclopentadienyl)-iodo-(3-methyl-4-phenyl-1-propyl-1H-1,2,3-triazol-3-ium-5-yl)nickel
(3c)

The starting materials used: 3-methyl-4-phenyl-1-propyl-1H-1,2,3-triazol-3-ium iodide (0.80 g, 2 mmol) and $NiCp_2$ (0.46 g, 2.43 mmol). Reddish crystalline product (0.49 g, 63%). Crystals suitable for X-ray crystallography were grown by layering hexane on dichloromethane. ^{1}H NMR ($CDCl_3$ 400 MHz): δ 7.66-7.83 (bm, Ar), 5.15 (s, Cp), 4.35 (s, N-CH_3), 4.70 (m, CH_2), 2.14-2.19 (m, CH_2), 1.11 (s, CH_3). ^{13}C NMR ($CDCl_3$, 400 MHz): δ 148.0, 130.5, 129.8, 129.7, 128.8, 128.6, 91.5, 57.7, 37.1, 23.3, 11.3. IR ν_{max} (cm^{-1}): 3439(m), 3350(m), 2987 (m), 1608 (s), 1579 (m), 1483 (s), 1464 (s), 1433 (s), 1345 (s), 1227 (m), 1073 (s), 1045 (m), 765 (s), 691 (s), 508 (s). HRMS (ESI) m/z for $C_{17}H_{20}N_3Ni$ [M-I]: calculated: 324.1011, found: 324.1071.

(η^5-Cyclopentadienyl)-iodo-(1-benzyl-3-methyl-4-phenyl-1H-1,2,3-triazol-3-ium-5-yl)nickel
(3d)

The starting materials used: 1-benzyl-3-methyl-4-phenyl-1H-1,2,3-triazol-3-ium iodide (0.71 g, 1.88 mmol) and $NiCp_2$(0.35 g, 1.88 mmol). Reddish solid product (0.50 g, 63%).Crystals suitable for X-ray crystallography were grown by layering hexane on dichloromethane. ^{1}H NMR ($CDCl_3$ 400 MHz): δ 7.26-8.19 (bm, Ar), 4.82(s, Cp), 4.35(s, N-CH_3), 4.02 (s, CH_2); ^{13}C NMR ($CDCl_3$ 400 MHz): δ 130.7, 129.9, 129.8, 128.9, 128.8, 125.8, 125.4, 120.5, 91.8, 61.4, 37.5. 1. IR νmax (cm^{-1}): 3433(b), 2927 (m), 1695 (s), 1622 (m), 1450 (s), 1338 (s), 1073(s), 780 (m), 727 (s), 694(m), 698 (s). HRMS (ESI) m/z for $C_{21}H_{20}N_3Ni$ [M-I]: calculated: 372.1011, found: 372.0851.

Oxidation reaction of n*-octane with compounds 3a-d as catalysts*

The oxidants H_2O_2 (30%) and *t*-BuOOH (70%) were respectively purchased from Sigma-Aldrich and DLD Scientific and used as supplied. The reagents utilised for the calibration of the GC: 1-octanol (99%), 2-octanol (97%), 3-octanol (98%), 4-octanone (99%), octanal (99%) and octanoic acid (99%) were obtained from Sigma-Aldrich, 2-octanone (98%), 3-octanone (97%), 4-octanol (98%) and *n*-octane (99%) were sourced from Fluka, and pentanoic acid (98%) from Merck. When required, double distilled water was used.

A typical oxidation reaction was carried out in a 2-neck round bottom flask fitted with an efficient reflux condenser operating under an atmosphere of nitrogen as follows: the catalyst (as indicated) and substrate were dissolved in dry solvent acetonitrile (CH_3CN), then an aqueous solution of H_2O_2 (or t-BuOOH) was added and stirred vigorously at indicated temperature and time. Except for studies on the optimisation of temperature and time, all the reactions were conducted at 80 °C and 24 h respectively. The product was analysed by after the required time period, an aliquot of sample was removed using a Pasteur pipette and filtered through a cotton wool plug, after which 0.5 μL of the aliquot was injected into the GC for analysis and quantification.

In all samples, excess solid triphenylphosphine (PPh_3) was added in order to capture alkyl hydroperoxides (if present) which are known to gradually decompose into corresponding ketones (aldehydes) and alcohols in the hot injector and columns [46,47]. A typical chromatogram is shown in the supplementary information section (Fig. S20).

Total conversion was calculated as total moles of product/initial moles of substrate while selectivity was calculated as moles of product/total moles of product and both were expressed as a percentage. 2,4,6-trichlorobenzene was used as the internal standard and all experiments were conducted in an Agilent Technology 6820

Please cite this article in press as: S.G. Mncube, M.D. Bala, Application of 1,2,3-triazolylidene nickel complexes for the catalytic oxidation of *n*-octane, Mol. Catal. (2017), http://dx.doi.org/10.1016/j.mcat.2017.03.005

GC System equipped with a flame ionization detector (FID) and an Agilent DB-Wax column with a length of 30 meters, inner diameter of 0.25 mm and a thickness of 0.25 mm.

X-ray structure determination

Single crystals were selected and glued onto the tip of a glass fibre, mounted in a stream of cold nitrogen at 173 K and centred in the X-ray beam using a video camera. Intensity data were collected on a Bruker APEX II CCD area detector diffractometer with graphite monochromated Mo Kα radiation (50 kV, 30 mA) using the APEX 2 data collection software. The collection method involved ω-scans of width 0.5° and 512 × 512 bit data frames. Data reduction was carried out using the program SAINT+ while face indexed and multi-scan absorption corrections were made using SADABS. The structures were solved by direct methods using SHELXS [48]. Non-hydrogen atoms were first refined isotropically followed by anisotropic refinement by full matrix least-squares calculations based on F2 using SHELXS. Hydrogen atoms were first located in the difference map then positioned geometrically and allowed to ride on their respective parent atoms. Diagrams were generated using SHELXTL, PLATON [49] and ORTEP-3 [50]. Crystallographic data for the structures in this article have been deposited with the Cambridge Crystallographic Data Centre, CCDC 1457104-1457105 for 3c-d respectively. These data can be obtained free of charge at http://www.ccdc.cam.ac.uk/conts/retrieving.html (or from the Cambridge Crystallographic Data Centre, 12 Union Road Cambridge CB2 1EZ, UK; Fax: +44 1223/336 033; E mail: deposit@ccdc cam ac uk

Acknowledgements

We are grateful to the Centre of Excellence in Catalysis (c* change, project PAR08), the NRF and UKZN for generous financial support. We thank Dr Bernard Omondi and Mr Sizwe Zamisa for X-ray crystallographic data collection and refinement.

Appendix A. Supplementary data

Supplementary data associated with this article can be found, in the online version, at http://dx.doi.org/10.1016/j.mcat.2017.03.005.

References

[1] W. Kirmse, Angew. Chem. Int. Ed. 49 (2010) 8798–8801.
[2] J.D. Crowley, A.L. Lee, K.J. Kilpin, Aust. J. Chem. 64 (2011) 1118–1132.
[3] E. Peris, R.H. Crabtree, C. R. Chim. 6 (2003) 33–37.
[4] F.E. Hahn, M.C. Jahnke, Angew. Chem. Int. Ed. 47 (2008) 3122–3172.
[5] A. Monney, E. Alberico, Y. Ortin, H. Muller-Bunz, S. Gladiali, M. Albrecht, Dalton Trans. 41 (2012) 8813–8821.
[6] A. Binobaid, M. Iglesias, D. Beetstra, A. Dervisi, I. Fallis, K.J. Cavell, Eur. J. Inorg. Chem. 34 (2010) 5426–5431.
[7] R.A. Kelly III, H. Clavier, S. Giudice, M. Scott, E.D. Stevens, J. Bordner, I. Samardjiev, C.D. Hoff, L. Cavallo, S.P. Nolan, Organometallics 27 (2008) 202–210.
[8] K.F. Donnelly, A. Petronilho, M. Albrecht, Chem. Commun. 47 (2013) 1145–1159.
[9] B.M.J.M. Suijkerbuijk, B.N.H. Aerts, H.P. Dijkstra, M. Lutz, A.L. Spek, G.V. Koten, R.J.M.K. Gebbink, Dalton Trans. (2007) 1273–1276.
[10] R.J. Detz, S. ArevaloHeras, R. de Gelder, P.W.N.M. van Leeuwen, H. Hiemstra, J.N.H. Reek, J.H.V. Maarseveen, Org. Lett. 8 (2006) 3227–3230.
[11] G. Guisado-Barrios, J. Bouffard, B. Donnadieu, G. Bertrand, Angew. Chem. Int. Ed. 28 (2010) 4759–4762.
[12] A. Poulain, D. Canseco-Gonzalez, R. Hynes-Roche, H. Muller-Bunz, O. Schuster, H. Stoeckli-Evans, A. Neels, M. Albrecht, Organometallics 30 (2011) 1021–1029.
[13] C.D. Abernethy, A.H. Cowley, R.A. Jones, J. Organomet. Chem. 596 (2000) 3–5.
[14] P. Mathew, A. Neels, M. Albrecht, J. Am. Chem. Soc. 130 (2008) 13534–13535.
[15] T. Karthikeyan, S. Sankararaman, Tetrahedron Lett. 50 (2009) 5834–5837.
[16] H.L.N. Lebel, M.K. Janes, A.B. Charette, S.P. Nolan, J. Am. Chem. Soc. 126 (2004) 5046–5047.
[17] R. Lalrempuia, N.D. McDaniel, H. Mueller-Bunz, S. Bernhard, M. Albrecht, Angew. Chem. Int. Ed. 49 (2010) 9765–9768.
[18] J. Kaeobamrung, J.W. Bode, Org. Lett. 11 (2009) 677–680.
[19] D.S. McGuiness, K.J. Cavell, Organometallics 19 (2000) 741–748.
[20] S. Rostamnia, H.G. Hossieni, E. Doustkhah, J. Organomet. Chem. 791 (2015) 18–23.
[21] S. Rostamnia, E. Doustkhah, R. Bulgar, B. Zeynizadeh, Micropor. Mesopor. Mater. 225 (2016) 272–279.
[22] A. Fürstner, O.R. Thiel, L. Ackermann, H.-J. Schanz, S.P. Nolan, J. Org. Chem. 65 (2000) 2204–2207.
[23] R.A. Periana, G. Bhalla, W.J. Tenn III, K.J.H. Young, X.Y. Liu, O. Mironov, C.J. Jones, V.R. Ziatdinov, J. Mol. Catal. A: Chem. 220 (2004) 7–25.
[24] D. Munz, T. Strassner, Inorg. Chem. 54 (2015) 5043–5052.
[25] L. Soobramoney, M.D. Bala, H.B. Friedrich, Dalton Trans. 43 (2014) 15968–15978.
[26] S.G. Mncube, M.D. Bala, J. Mol. Liq. 215 (2016) 396–401.
[27] E. Kadwa, M.D. Bala, H.B. Friedrich, Appl. Clay Sci. 95 (2014) 340–347.
[28] P. Li, L. Wang, Lett. Org. Chem. 4 (2007) 23–26.
[29] Z. Yacob, J. Shah, J. Leistner, J. Liebscher, Synlett 15 (2008) 2342–2344.
[30] Y. Wei, A. Petronilho, H. Mueller-Bunz, M. Albrecht, Organometallics 33 (2014) 5834–5844.
[31] W. Buchowicz, W. Wojtczak, A. Pietrzykowski, A. Lupa, L.B. Jerzykiewicz, A. Makal, K. Wozíniak, Eur. J. Inorg. Chem. 43 (2010) 648–656.
[32] W. Buchowicz, A. Koziol, L.B. Jerzykiewicz, T. Lis, S. Pasynkiewicz, A. Pecherzewska, A. Pietrzykowski, J. Mol. Catal. A: Chem. 257 (2006) 118–123.
[33] A. Wada, S. Ogo, S. Nagatomo, T. Kitagawa, Y. Watanabe, K. Jitsukawa, H. Masuda, Inorg. Chem. 41 (2002) 616–618.
[34] K. Nikki, H. Inakura, N. Wu-Le, T.J. Suzuki, Endo Chem. Soc. Perkin Trans. 2 (2001) 2370–2373.
[35] G.B. Shul'pin, T. Sooknoi, V.B. Romakh, G. Süss-Fink, L.S. Shul'pina, Tetrahedron Lett. 47 (2006) 3071–3075.
[36] G.B. Shul'pin, G. Süss-Fink, L.S. Shul'pina, J. Mol. Catal. A: Chem. 170 (2001) 17–34.
[37] M.V. Kirillova, A.M. Kirillov, D. Mandelli, W.A. Carvalho, A.J.L. Pombeiro, G.B. Shul'pin, J. Catal. 272 (2010) 9–17.
[38] L.S. Shul'pina, M.V. Kirillova, A.J.L. Pombeiro, G.B. Shul'pin, Tetrahedron 65 (2016) 2424–2429.
[39] D. Mandelli, K.C. Chiacchio, Y.N. Kozlov, G.B. Shul'pin, Tetrahedron Lett. 49 (2008) 6693–6697.
[40] T.C.O.M. Leod, M.V. Kirillova, A.J.L. Pombeiro, M.A. Schiavon, M.D. Assis, Appl. Catal A 372 (2010) 191–198.
[41] G.B. Shul'pin, T. Sooknoi, V.B. Romakh, G. Süss-Fink, L.S. Shul'pina, Tetrahedron Lett. 47 (2006) 3071–3075.
[42] V.B. Romakh, B. Therrien, G. Süss-Fink, G.B. Shul'pin, Inorg. Chem. 46 (2007) 1315–1321.
[43] Y. Wei, A. Petronilho, H. Mueller-Bunz, M. Albrecht, Organometallics 33 (2014) 5834–5844.
[44] S.M. Yiu, W.L. Man, T.C. Lau, J. Am. Chem. Soc. 130 (2008) 10821–10827.
[45] J.T. Fletchera, J.E. Reillya, Tetrahedron Lett. 52 (2011) 5512–5515.
[46] G.B. Shul'pin, J. Mol. Catal. A: Chem. 189 (2002) 39–66.
[47] G.B. Shul'pin, Mini-Rev. Org. 6 (2009) 95–104.
[48] G.M. Sheldrick, Acta Crystallogr. Sect. A: Fundam. Crystallogr. 64 (2008) 112–122.
[49] A.L. Spek, J. Appl. Crystallogr. 36 (2003) 7–13.
[50] L.J. Farrugia, J. Appl. Crystallogr. 30 (1997) 565–566.

Please cite this article in press as: S.G. Mncube, M.D. Bala, Application of 1,2,3-triazolylidene nickel complexes for the catalytic oxidation of *n*-octane, Mol. Catal. (2017), http://dx.doi.org/10.1016/j.mcat.2017.03.005